



# Hourly elemental concentrations in PM<sub>2.5</sub> aerosols sampled simultaneously at urban background and road site during SAPUSS – diurnal variations and PMF receptor modelling

M. Dall'Osto<sup>1</sup>, X. Querol<sup>1</sup>, F. Amato<sup>2</sup>, A. Karanasiou<sup>1,3</sup>, F. Lucarelli<sup>4</sup>, S. Nava<sup>4</sup>, G. Calzolari<sup>4</sup>, and M. Chiari<sup>4</sup>

<sup>1</sup>Institute of Environmental Assessment and Water Research, Spanish Research Council (IDAEA-CSIC), c/Jordi Girona 18–26, 08034 Barcelona, Spain

<sup>2</sup>TNO, Built Environment and Geosciences, Dept. of Climate, Air and Sustainability, Utrecht, the Netherlands

<sup>3</sup>Centre for Research in Environmental Epidemiology (CREAL), Barcelona, Spain

<sup>4</sup>Department of Physics and Astronomy, University of Florence and National Institute of Nuclear Physics (INFN), via Sansone 1, 50019 Sesto Fiorentino, Italy

Correspondence to: M. Dall'Osto (manuel.dalosto@gmail.com)

Received: 30 July 2012 – Published in Atmos. Chem. Phys. Discuss.: 13 August 2012

Revised: 2 April 2013 – Accepted: 4 April 2013 – Published: 26 April 2013

**Abstract.** Hourly-resolved aerosol chemical speciation data can be a highly powerful tool to determine the source origin of atmospheric pollutants in urban environments. Aerosol mass concentrations of seventeen elements (Na, Mg, Al, S, Cl, K, Ca, Ti, V, Cr, Mn, Fe, Ni, Cu, Zn, Sr and Pb) were obtained by time (1 h) and size (PM<sub>2.5</sub> particulate matter < 2.5 μm) resolved aerosol samples analysed by Particle Induced X-ray Emission (PIXE) measurements. In the Marie Curie European Union framework of SAPUSS (Solving Aerosol Problems by Using Synergistic Strategies), the approach used is the simultaneous sampling at two monitoring sites in Barcelona (Spain) during September–October 2010: an urban background site (UB) and a street canyon traffic road site (RS). Elements related to primary non-exhaust traffic emission (Fe, Cu), dust resuspension (Ca) and anthropogenic Cl were found enhanced at the RS, whereas industrial related trace metals (Zn, Pb, Mn) were found at higher concentrations at the more ventilated UB site. When receptor modelling was performed with positive matrix factorization (PMF), nine different aerosol sources were identified at both sites: three types of regional aerosols (regional sulphate (S) – 27 %, biomass burning (K) – 5 %, sea salt (Na-Mg) – 17 %), three types of dust aerosols (soil dust (Al-Ti) – 17 %, urban crustal dust (Ca) – 6 %, and primary traffic non-exhaust brake dust (Fe-Cu) – 7 %), and three types of industrial aerosol plumes-like events (shipping oil combus-

tion (V-Ni) – 17 %, industrial smelters (Zn-Mn) – 3 %, and industrial combustion (Pb-Cl) – 5 %, percentages presented are average source contributions to the total elemental mass measured). The validity of the PMF solution of the PIXE data is supported by very good correlations with external single particle mass spectrometry measurements. Some important conclusions can be drawn about the PM<sub>2.5</sub> mass fraction simultaneously measured at the UB and RS sites: (1) the regional aerosol sources impact both monitoring sites at similar concentrations regardless their different ventilation conditions; (2) by contrast, local industrial aerosol plumes associated with shipping oil combustion and smelters activities have a higher impact on the more ventilated UB site; (3) a unique source of Pb-Cl (associated with combustion emissions) is found to be the major (82 %) source of fine Cl in the urban agglomerate; (4) the mean diurnal variation of PM<sub>2.5</sub> primary traffic non-exhaust brake dust (Fe-Cu) suggests that this source is mainly emitted and not resuspended, whereas PM<sub>2.5</sub> urban dust (Ca) is found mainly resuspended by both traffic vortex and sea breeze; (5) urban dust (Ca) is found the aerosol source most affected by land wetness, reduced by a factor of eight during rainy days and suggesting that wet roads may be a solution for reducing urban dust concentrations.

## 1 Introduction

It has been largely recognised that air quality and exposure to air pollution have severe consequences and direct growing effects on human health such as diseases of the respiratory and cardiac systems (Pope and Dockery, 2006). The effects have become of great interest in urban areas where the population density and human activities are highly concentrated. The sources of  $\text{PM}_{2.5}$  ( $\text{PM} < 2.5 \mu\text{m}$ ; fine particles) and  $\text{PM}_{2.5-10}$  ( $\text{PM} 2.5-10 \mu\text{m}$ ; coarse particles) usually differ and they include a wide range of natural phenomena and human activities. Typically, the fine particles are produced from combustion processes, forest fires and transformations of gaseous species, whereas coarser ones originate from sea salt, constructions/demolitions, non-exhaust vehicle emissions. Contradicting theories exist as to whether fine or coarse PM produces health effects (Brunekreef and Holgate, 2002; Brunekreef and Forsberg, 2005). However, the size cut at  $2.5 \mu\text{m}$  does not separate compositions from main different sources well and several studies show that  $\text{PM}_1$  ( $\text{PM} < 1 \mu\text{m}$ ) would be far more effective at separating particles from these sources which produce drastically different compositions (Pastor et al., 2003; Amato et al., 2009). In other words, the  $\text{PM}_{2.5}$  fraction lying between the  $\text{PM}_1$  and the  $\text{PM}_{10}$  ones is the most difficult to characterise as composed of a large variety of aerosol sources. In the European Union, the Clean Air for Europe (CAFE) establishes that a  $\text{PM}_{2.5}$  annual limit value of  $25 \mu\text{g m}^{-3}$  must be reached by January 2015 (EEA, 2010). A detailed knowledge of the chemical composition of particles – alongside knowledge of their size and concentration – is important to apportion the sources of PM in the atmosphere. The vast majority of aerosol source apportionment studies in the literature are limited by the time resolution of the input samples, typically off-line filter collections of 12–24 h (Pant and Harrison, 2012). This is due to a number of reasons, including the air flow rate of the sampler and the detection limit of the analytical method to be applied on the collected aerosol mass. However, the impact on PM levels and personal exposure of many sources like industries or vehicular traffic as an emission source is more evident on an hourly time basis. Furthermore, source apportionment receptor models need a series of samples containing material from the same set of sources in differing proportions. Increasing the time resolution of the measurements typically provides samples that have greater between-sample variability in the source contributions than samples integrated over longer time periods.

For this purpose, in this study we performed measurements with the PIXE technique, providing hourly elemental concentrations of the  $\text{PM}_{2.5}$  aerosol mass loadings. The hourly resolution allows us to ensure a better reliability of the receptor modelling results. Furthermore, it is possible to obtain very accurate aerosol source profiles which can, therefore, be used as a reference data and as a constrains for the

data analysis of other less defined data obtained at lower time resolution (12–24 h).

PIXE offers very high sensitivities, thus, allowing the use of samplers with high time and size resolution (Lucarelli et al., 2011). This study is part of the SAPUSS (Solving Aerosol Problems by Using Synergistic Strategies) project, involving concurrent measurements of aerosols with multiple techniques occurring simultaneously (Dall'Osto et al., 2012). The aim of the present study is to monitor the elemental concentrations simultaneously measured at a Road Site (RS) and at an Urban Background (UB) site during a four-week campaign. The road increments (road concentrations minus urban background concentrations) are investigated as well as other differences found among the two sites. Furthermore, positive matrix factorization (PMF) analysis is carried out, and particular emphasis is given in describing the contribution of different sources between the two monitoring sites. Previous work in the same Western Mediterranean Basin (WMB) region by using similar techniques focused on  $\text{PM}_{10}$  trace metals variations in urban areas and regional surrounding (Moreno et al., 2011), on  $\text{PM}_{10}$  roadside enrichment of atmospheric particulate pollutants (Amato et al., 2011) and on the air quality benefit of street clean activities (Amato et al., 2010). The novelty of this study stands in the analysis of simultaneous  $\text{PM}_{2.5}$  aerosols data collected at the UB and RS SAPUSS monitoring sites, in the application of PMF receptor modelling to the hourly data in order to identify different aerosol sources, and in the comparison of such results with the ones obtained by two Aerosol Time-of-Flight Mass Spectrometers (ATOFMSs). Special emphasis is given in describing all detected elements and their association to regional and local aerosol sources, including different types of road dust and unique anthropogenic plumes of oil combustion, trash burning and industrial activities.

## 2 Methods

### 2.1 Location

The SAPUSS campaign (Dall'Osto et al., 2012) was carried out mainly in Barcelona, a city located in the WMB in the North East (NE) part of Spain. The sampling campaign took part between 20 September and 20 October 2010 (local time, UCT+2). The unique SAPUSS approach involved a large variety of instrumentation deployed simultaneously in a number of monitoring sites (six), but the PIXE analysis was carried out only at the two SAPUSS supersites:

- Road site (RS) was situated in a car park next to a major road (Carrer Urgell). The road, which cuts the city from South East to North West, is a street canyon composed by a two-way cycling path and a one-way four lane vehicle road. Vehicle intensity for the month of measurements was about 17 000 vehicles per day.

- Urban Background site (UB) was situated at the North Western periphery of the city centre in a small park. It is important to note that a main road (Avenida Diagonal, 127 000 vehicles day<sup>-1</sup>) is located about 500 m away from the site.

The two sites were about 2 km away from each other (Dall'Osto et al., 2012). However, whilst the wind can impact the UB site at all directions, the RS urban street canyons characteristic reduce natural ventilations. In other words, the mechanically generated wind flow and turbulence at the RS are the results of combined processes of atmospheric wind and vehicular traffic.

## 2.2 Instrumentation

A compact and versatile sampler which collects hourly samples on a unique frame (the two-stages, continuous streaker sampler) was deployed. The sampling devices (Prati et al., 1998) are designed to separate the fine (< 2.5 µm) and the coarse (2.5–10 µm) size fractions of aerosol particles. A pre-impactor removes particles with aerodynamic diameter above 10 µm, a paraffin-coated Kapton foil is used as an impaction surface for coarse particles and a Nuclepore filter as a fine particle collector. The rotation speed of the two collecting plates during sampling, the pumping orifice width and the beam size we used for the subsequent analysis are such that an overall resolution of about 1 h is obtained on the elemental composition of air particulate. A detailed description of the instrumentation can be found elsewhere (Prati et al., 1998; Lucarelli et al., 2011). PIXE analyses was performed with 3 MeV protons from the 3 MV Tandem accelerator of the LABEC laboratory of INFN in Florence, with the external beam set-up extensively described elsewhere (Chiari et al., 2005; Calzolari et al. 2006). The beam (30–80 nA) scanned the streak in steps corresponding to 1 h of aerosol sampling; each spot was irradiated for about 180 s. PIXE spectra were fitted using the GUPIX software package and elemental concentrations were obtained via a calibration curve from a set of thin standards of known areal density. The accuracy of hourly elemental concentrations was determined by a sum of independent uncertainties on: standard samples thickness (5 %), aerosol deposition area (2 %), air flow (2 %) and X-rays counting statistics (2–20 %). Detection limits were about 10 ng m<sup>-3</sup> for low-Z elements and 1 ng m<sup>-3</sup> for medium-high Z elements. The following elements were detected: Na, Mg, Al, P, S, Cl, K, Ca, Ti, V, Cr, Mn, Fe, Ni, Cu, Zn, Sr and Pb. Unfortunately Nuclepore filters were contaminated by Si and Br whose concentrations were not possible to determine. During SAPUSS, hourly data were collected between 27 September 2010 and 18 October 2010 for a total of 506 h. Data coverage during this period was 82 % at the UB and 62 % at the RS. The overlap between the two sites was higher than 98 %, making 62 % of the time having simultaneous measurements. It is important to note

that only the fine PM<sub>2.5</sub> fraction data analysis is reported in this study.

Elemental mass concentrations obtained by PIXE were compared to daily filter measurements collected during SAPUSS (Dall'Osto et al., 2012). Briefly, PM<sub>2.5</sub> daily mass concentrations (24 h time resolution) were determined by standard gravimetric procedures and analyzed following the procedures described by Querol et al. (2001): Al, Ca, K, Mg, Fe, Ti, Mn, P, S, Na and 25 trace elements by conventional methods including inductively coupled plasma atomic emission spectrometry and mass spectrometry (ICP-AES and ICP-MS, respectively, Dall'Osto et al., 2012). Accordingly, the hourly PIXE data were binned into 24 h intervals.

## 2.3 PMF analysis

The source identification analysis of the PIXE data was carried out by PMF, and both datasets (UB and RS) were analysed simultaneously. In other words, the PMF analysis was carried out on one large dataset (sum of UB and RS), so the resulting common aerosol sources could be compared between the two monitoring sites. Out of the 18 elements presented in Sect. 2.2, Sr was not used in the PMF analysis as often below detection limit. The total number of hours with PIXE data available for the UB and RS datasets were 318 and 444, respectively. The two datasets were merged together resulting in a 762 rows (time; hours between between 27 September 2010 and 18 October 2010) by 17 columns (element concentrations). By doing so, we assume that the chemical profiles of the resolved sources do not change between the two nearby sampling sites (2 km apart from each other).

To our knowledge, this is the first time such a study is being attempted. However, it is important to recognise that only the PIXE data are used in this receptor modelling studies, leaving out important components including organic (organic carbon), elemental carbon and inorganic species (nitrate, ammonium, etc.). One aim of the present study is to test the capability of the hourly PIXE data to capture different aerosol sources. Given the fact that some aerosol sources may show a temporal variation of only few hours, this study could reveal unique aerosol sources not identified with a dataset composed of a larger variety of chemical species collected at a lower (daily) time resolution. On the other hand, future SAPUSS receptor modelling studies will focus on combined hourly data obtained from different types of particle mass spectrometers (Dall'Osto et al., 2012).

The Polissar et al. (1998) procedure was used to choose the data and their associated uncertainties as the PMF input data. PMF solutions from 5 to 10 factors were systematically explored (also changing the FPEAK value) and the resulting Q values, the scaled residuals, and the F and G matrices were examined to find the most reasonable solution. Finally, the solution with nine sources and PEAK=0 was the most reasonable. The scaled residuals (Paatero and Hopke, 2003)

**Table 1.** Intercomparison between PIXE and ICP-MS/ICP-AES techniques; average hourly elemental concentrations and minimum and maximum hourly and daily values for the elements detected by PIXE during the SAPUSS field study. (N.A. Not available due to limited number of points).

Element	Inter comparison with ICP-MS/ICP-AES techniques. Regression line are Y (PIXE analysis) and X (ICP-MS/ICP-AES)		PIXE average hourly concentrations [ $\text{ng m}^{-3}$ ]			PIXE maximum and minimum values (H= hourly; D= daily) [ $\text{ng m}^{-3}$ ]	
	UB	RS	UB	RS	diff RS – UB (%)	UB	RS
Na	$Y = 0.85 X (R^2 = 0.44)$	$Y = 1.1 X (R^2 = 0.41)$	$430 \pm 160$	$400 \pm 220$	Not. Sign.	(32–1016)H (130–612)D	(68–1295)H (154–490)D
Mg	$Y = 0.78 X (R^2 = 0.55)$	$Y = 1.25 X (R^2 = 0.8)$	$43 \pm 16$	$47 \pm 23$	Not. Sign.	(22–106)H (29–81)D	(24–143)H (32–68)D
Al	$Y = 0.88 X (R^2 = 0.87)$	$Y = 0.70 X (R^2 = 0.45)$	$50 \pm 24$	$45 \pm 30$	Not. Sign.	(15–146)H (41–130)D	(2.3–181)H (34–64)D
S	$Y = 0.80 X (R^2 = 0.91)$	$Y = 0.80 X (R^2 = 0.88)$	$669 \pm 460$	$620 \pm 320$	Not. Sign.	(103–4126)H (308–1230)D	(116–1607)H (236–882)D
Cl	N.A.	N.A.	$50 \pm 34$	$71 \pm 79$	29	(17–304)H (19–59)D	(2.5–532)H (39–91)D
K	$Y = 0.85 X (R^2 = 0.30)$	$Y = 0.86 X (R^2 = 0.6)$	$89 \pm 39$	$82 \pm 30$	Not. Sign.	(25–214)H (54–201)D	(20–178)H (56–102)D
Ca	N.A.	$Y = 1.15 X (R^2 = 0.60)$	$109 \pm 86$	$130 \pm 149$	17	(25–665)H (53–126)D	(21–817)H (43–294)D
Ti	N.A.	N.A.	$11 \pm 3$	$12 \pm 4$	Not. Sign.	(8.1–23)H (20–20)D	(8.0–29)H (8.0–13)D
V	N.A.	$Y = 0.80 X (R^2 = 0.20)$	$9 \pm 3$	$8 \pm 3$	Not. Sign.	(5.6–17)H (7.0–13)D	(5.5–16)H (6.1–10)D
Cr	N.A.	N.A.	$8 \pm 2$	$8 \pm 2$	Not. Sign.	(3.8–16)H (4.0–12)D	(3.8–16)H (4.7–10)D
Mn	$Y = 1.35 X (R^2 = 0.40)$	$Y = 1.2 X (R^2 = 0.55)$	$7 \pm 7$	$6 \pm 5$	–17	(2.5–51)H (4.0–9.0)D	(2.5–27)H (3.1–7.2)D
Fe	$Y = 1.2 X (R^2 = 0.7)$	$Y = 0.90 X (R^2 = 0.7)$	$96 \pm 60$	$131 \pm 94$	27	(2.2–303)H (43–155)D	(15–525)H (54–171)D
Ni	$Y = 0.82 X (R^2 = 0.4)$	$Y = 0.89 X (R^2 = 0.7)$	$3 \pm 1$	$3 \pm 1$	Not. Sign.	(1.1–7.6)H (2.0–5.0)D	(1.0–7.1)H (1.6–4.2)D
Cu	$Y = 0.90 X (R^2 = 0.65)$	$Y = 0.80 X (R^2 = 0.7)$	$5 \pm 3$	$8 \pm 4$	20	(1.2–16)H (2.0–8.0)D	(1.7–22)H (2.9–7.5)D
Zn	$Y = 0.7 X (R^2 = 0.65)$	$Y = 0.75 X (R^2 = 0.75)$	$35 \pm 56$	$25 \pm 31$	–41	(2.8–377)H (19–55)D	(2.6–249)H (6.3–57)D
Sr	N.A.	N.A.	$2 \pm 1$	$2 \pm 1$	Not. Sign.	(1.4–4.0)H (1.6–3.0)D	(1.4–3.0)H (1.4–2.2)D
Pb	$Y = 0.85 X (R^2 = 0.40)$	$Y = 0.95 X (R^2 = 0.80)$	$17 \pm 9$	$12 \pm 5$	–42	(4.0–41)H (3.4–14)D	(4.5–18)H (5.7–12)D

were almost normally distributed and between  $\pm 3$  for the majority of the species. Finally, it is important to note that the validity of the PMF solution was further supported by correlation with external measurements taken during the SAPUSS, as discussed in Sect. 4.

### 3 Results

According to earlier studies, the ambient  $\text{PM}_{2.5}$  concentrations (annual average at urban background: 2003–2006) in Barcelona were in the ranges of  $25\text{--}29 \mu\text{g m}^{-3}$ , although a reduction has been noticed in the last 2007–2011 period ( $17\text{--}20 \mu\text{g m}^{-3}$ , Reche et al., 2011) as a result of air quality mitigations and financial crisis. During the SAPUSS, average concentrations of  $\text{PM}_{2.5}$  were  $18.6 \pm 4 \mu\text{g m}^{-3}$  and

$16.2 \pm 3 \mu\text{g m}^{-3}$  at the RS and UB, respectively (Dall'Osto et al., 2012).

#### 3.1 Overview of $\text{PM}_{2.5}$ elements concentrations detected by the PIXE

##### 3.1.1 $\text{PM}_{2.5}$ Inter comparison between PIXE data and other analytical techniques (ICP-MS/ICP-AES techniques)

Table 1 shows linear regression as Y for PIXE data analysis and X for ICP-MS/ICP-AES data, respectively. It displays the overall good comparison of daily filters measurements and daily PIXE data (averaged from the hourly data) for the  $\text{PM}_{2.5}$  mass concentrations within 30 % for Na, Mg, Al, S, K, Mn, Fe, Ni, Cu, Zn and Pb for both UB and RS sites. Some missing data and/or low elemental concentrations

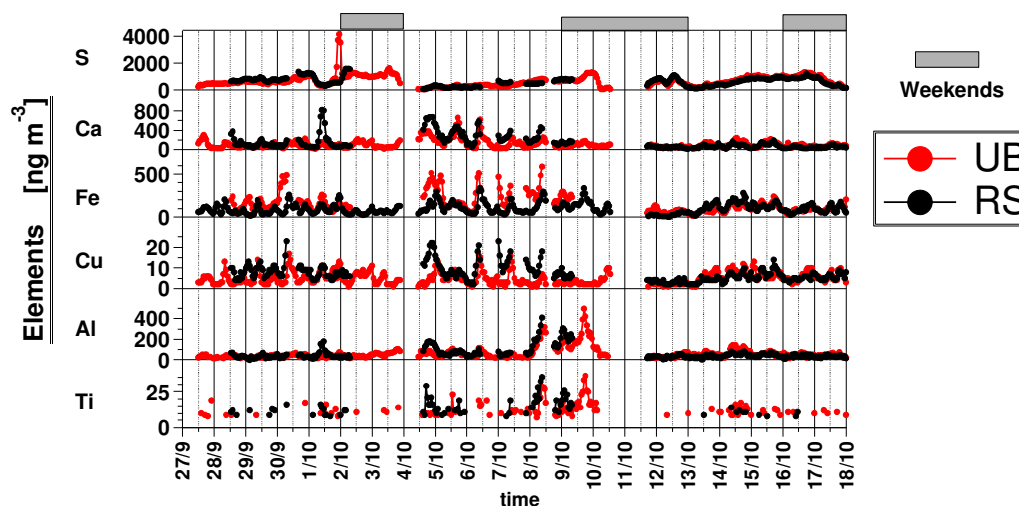


**Fig. 1.** Temporal trends (all in  $\text{ng m}^{-3}$ ) of selected elements measured simultaneously at the UB and RS sites.

did not allow a full intercomparison: Ca and V (also within 30 %) were only available at the RS site. By contrast, limited number of data points and lack of temporal overlaps did not allow comparing Cl, Ti, Cr and Sr at both sites (Table 1). Overall, this study is in line with previous ones, supporting a fair correlation between PIXE and ICP-MS/ICP-AES based techniques, sampled at hourly and daily resolution, respectively (Richard et al., 2011; Moreno et al., 2011; Amato et al., 2011).

### 3.1.2 Average concentrations and site inter comparison

Table 1 presents an overview of the mean elemental concentrations ( $\pm 1\sigma$ ) measured at both UB and RS sites. Average detected  $\text{PM}_{2.5}$  mass concentration for UB and RS was  $1.52 \mu\text{g m}^{-3}$  and  $1.64 \mu\text{g m}^{-3}$  (respectively), with a slightly higher total concentration (8 %) at the RS. Most elements (10 of the monitored 17) did not present statistically significant differences in concentrations between the UB and the RS site (Table 1, *t* test applied). S was found the most abundant element ( $640 \pm 350 \text{ ng m}^{-3}$ , averaged at both sites), characterised by a time component similar for most of the time at the two sampling sites and typical of secondary aerosols of regional origin. A spike in concentration was observed on 1 October between 8 p.m. and 12 p.m. only at the UB (Fig. 1). Na was found to be the second most abundant element at both sites at similar concentrations (Table 1). The mean Mg/Na ratio (0.13 at UB, 0.12 at RS) is typical of bulk sea-water ( $\text{Mg/Na}=0.12$ , Seinfeld and Pandis, 1998) and the percentage of Cl depletion was often above 90 %. The sea-salt Sulphur (ss-S) contribution was estimated to be on average 10 % in UB and 14 % in RS, respectively.

As far as the concentrations of soil related elements are concerned, some (Na, Mg, Al, K, Ti) did not present any enrichment in any of the two monitoring sites. By contrast,

higher concentrations of Ca (17 %), Fe (27 %) and Cu (20 %) were found at the RS relative to the UB. These increments are likely to be due to soil urban dust for Ca, and to non-exhaust primary traffic dust for Fe and Cu (Amato et al., 2011). The temporal patterns of Fe and Cu (Fig. 1) show a periodic behaviour with two peaks in coincidence with the traffic rush hours. Increased attention is focussing on non-exhaust emissions as exhaust emissions are progressively limited by regulations. Denier van der Gon et al. (2007) estimated that 50–75 % of the Cu emissions to the atmosphere in western Europe are due to brake wear. Several authors (Sternbeck et al., 2002; Gietl et al., 2010; Amato et al., 2011) also indicated Cu, Fe, Zn, and Ba as candidate marker metals for car non-exhaust sources, although a clear separation from industrial sources is not always possible. Moreover, it is worth reminding that some of these traffic related metals can be distributed mainly in the  $\text{PM}_{2.5-10}$  (coarse) size fraction, although a non-negligible fraction is also present in the finer ( $\text{PM}_{2.5}$  fraction).

The elemental ratios of soil related elements revealed different contributions of Al-Ti rich and Ca rich particle types. Figure 1 shows an increase in concentrations for Al and Ti during the period of 8–10 October 2010. This can also be seen in Fig. 2, where the Fe/Ca, Fe/Al, Ca/Al ratios changed from 1.07, 1.88, 2.15 during days affected by marine Polar air masses to 1.44, 0.80, 0.59 during Continental Tropical Saharan episodes (Dall'Osto et al., 2012). However, it is important to stress that such an episode was found to be moderate in relation to some previously reported Saharan dust intrusion in the SAPUSS study region (Chiari et al., 2005; Marenco et al., 2006). Indeed, the  $\text{PM}_{10}$  values recorded during the SAPUSS never exceeded the EU aerosol  $\text{PM}_{10}$  mass limits (Dall'Osto et al., 2012).

Some trace elements (V, Mn, Ni, Cu, Zn), usually associated with industrial emissions, were found to present similar

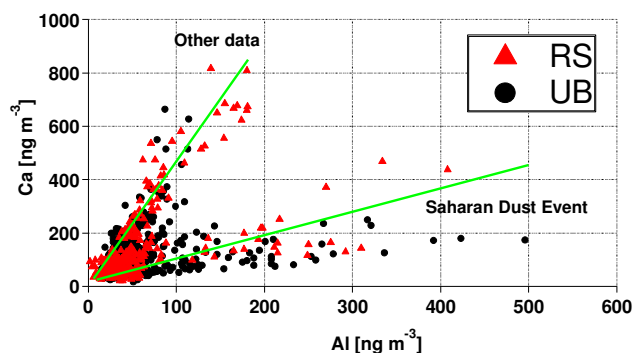


Fig. 2. Ca versus Al concentrations measured at the UB and RS site.

concentrations reported in previous studies (Pey et al., 2009; Amato et al., 2011; Moreno et al., 2011), whereas higher levels of Cr and Pb were recorded during this SAPUSS field study (Table 1). Trace metals related to industrial emission were found in higher concentrations at the UB site (Pb, Zn and Mn – 42 %, 41 % and 17 %, respectively – Table 1). The increment of Cl at the RS is also related to anthropogenic emissions, although a more in depth discussion is given in Sect. 3.2. Elevated  $\text{PM}_{2.5}$  Zn concentrations were previously reported in Barcelona, associated with Pb and attributed to emissions from smelters (Amato et al. 2009, 2011). Ni was found to be a complex multiple source pollutant, associated to industrial sources including stainless steel and residual oil combustion ones. V and Ni are usually the most abundant metals present in crude oil and most of their aerosol mass is usually attributed to shipping emissions (Pacyna and Pacyna, 2001; Moreno et al., 2010).

Some considerations on the maximum concentration values of the elements reported in Table 1 should be made. On average, hourly maximum concentrations values were 2.6 times higher than their daily average values (Table 1). Some metals presented maximum concentrations 3–5 times higher than their average (Ca, Mn, Fe), up to 8–10 (Mn, Zn). Hourly peak concentrations of Zn and Cu analysed by PIXE can reach maximum hourly levels as high as  $506 \text{ ngZn m}^{-3}$  and  $345 \text{ ngCu m}^{-3}$  when sampled in regions affected by strong industrial activities (De la Campa, 2011). Our study shows that the urban city of Barcelona can be impacted by industrial plumes of the same order of magnitude for Zn (max value  $377 \text{ ngZn m}^{-3}$ ).

It is important to note that these events with very high hourly concentrations can shift their total average concentration. Supplement Fig. S1 shows the frequency distributions of the hourly concentrations for both monitoring sites. When compared to the averages reported in Table 1, indeed lower average concentrations values are found for Gaussian distributions (Fig. S1) for Na, Ca, Mn and Zn relative to their arithmetic average (Table 1), implying that these four elements are particularly subjected to short temporal events with very high concentrations.

Table 2 shows the  $R^2$  correlation table (valid at  $p < 0.05$ , across all manuscript) obtained by comparing the temporal variation of the elemental concentrations simultaneously detected at the UB and RS sites. When the same element is compared between the two sites, some elements represent fairly good correlation: Na ( $R^2 = 0.63$ ), Mg ( $R^2 = 0.62$ ), Al ( $R^2 = 0.43$ ), Cl ( $R^2 = 0.55$ ), Ca ( $R^2 = 0.39$ ), Ti ( $R^2 = 0.40$ ) and Mn ( $R^2 = 0.51$ ). Sulphur showed a poor correlation ( $R^2 = 0.33$ ) between the two sites, but when the local UB event of 1 October was removed, the correlation increased to 0.75. Unexpectedly, other trace metals (V, Cr) usually associated with industrial and shipping emissions were found correlating only moderately well at the two sites although some others ones (Pb, Zn, Mn) did present some intra correlations at the two sites (Table 2). The reason is likely to be due to the limited natural ventilation of the RS site (a street canyon, a very typical condition in the urban agglomerate of Barcelona), impeding industrial plumes to disperse in the lower urban surface of the city (Solazzo et al., 2007). Another reason may lie in the fact that the spatial dimension of these industrial plumes may be smaller than the distance between the two monitoring sites, hence, impacting only part of the urban agglomerate of Barcelona. Fe and Cu were not found correlating with any other metals neither among the two different sites because of their local non-exhaust primary traffic emissions source.

### 3.1.3 Diurnal patterns

Due to the high time resolution of the PIXE data it was possible to detect the average diurnal variation of the elemental mass concentrations, and the most representative ones are displayed in Fig. 3. The diurnal temporal variation can be influenced by atmospheric mixing and dilution, effects of the planetary boundary layer mixing height, but also from the mere traffic pattern. Some elements did not present clear diurnal variation, indicating more of a regional rather than a local origin. For example, S presented similar diurnal profiles at both sites (Fig. 3a) and the divergence in the evening times at UB is due to a local spike event seen on 1 October. Mg (as well as Na and K) also presented modest variation during the day (Fig. 3b), suggesting additional regional sources (biomass burning and sea salt).

Ca and Al, two common element associated with mineral dust, presented different trends. Ca showed a strong morning peak likely to be due to traffic (Fig. 3c), but also an additional contribution in the afternoon likely to be due to the afternoon sea breeze enhancing dust resuspension. By contrast, Al did not show such a marked diurnal variation (Fig. 3d). Both Fe and Cu show a related pattern to the rush-hour times of increased traffic activity during morning (7–9 a.m.) and evening times (6–9 p.m., Fig. 3e–f). Mn and Pb were mainly seen during night time as industrial plumes impacting the city, probably due both to wind direction and industrial cycles. These seaward overnight industrial plumes are driven

**Table 2.** Inter-site correlation table ( $R^2$ ) of the 17 elements simultaneously detected at the UB and RS site. Poor correlations ( $R^2 < 0.25$ ) are not reported for clarity (–). Intra-site correlations were found generally poor, with only selected elements correlating within each other: Na, Mg ( $R^2 = 0.6$ ); Fe, Cu ( $R^2 = 0.7$ ); Zn, Cl, Pb, Cl ( $R^2 = 0.6$ ); Al, Ti ( $R^2 = 0.45$ ); K, S ( $R^2 = 0.4$ ) and Ni, V ( $R^2 = 0.5$ ).

$R^2$	Urban background (UB)																
	Na	Mg	Al	S	Cl	K	Ca	Ti	V	Cr	Mn	Fe	Ni	Cu	Zn	Sr	Pb
Road site (RS)	Na	0.62	0.4	–	–	–	–	–	–	–	0.33	–	–	–	–	–	–
	Mg	0.63	0.52	0.39	–	–	–	–	–	–	–	–	–	–	–	–	–
	Al	0.38	0.43	0.43	–	–	–	–	–	–	–	–	–	–	–	–	–
	S	–	–	–	0.33 (0.75)	–	–	–	–	–	–	–	–	–	–	–	–
	Cl	0.27	–	–	–	0.55	–	–	–	–	–	0.26	–	–	0.27	–	0.25
	K	0.39	0.37	0.45	–	–	–	–	–	–	–	–	–	–	–	–	–
	Ca	–	–	–	–	–	–	0.39	–	–	–	–	–	–	–	–	–
	Ti	–	0.41	0.61	–	–	0.34	–	0.4	–	–	–	–	–	–	–	–
	V	–	–	–	–	–	–	–	–	–	–	–	–	–	–	–	–
	Cr	–	–	–	–	–	–	–	–	–	–	–	–	–	–	–	–
	Mn	–	–	–	–	–	–	–	–	–	–	0.51	–	–	–	–	–
	Fe	–	–	–	–	–	–	–	–	–	–	–	–	–	–	–	–
	Ni	–	–	–	–	–	–	–	–	–	–	–	–	0.25	–	–	–
	Cu	–	–	–	–	–	–	–	–	–	–	–	–	–	–	–	–
	Zn	–	–	–	–	–	–	–	–	–	–	0.44	–	–	–	–	–
	Sr	0.4	0.3	–	–	–	–	–	0.26	0.39	0.35	–	–	–	–	–	–
	Pb	–	–	–	–	0.36	–	–	–	–	–	0.58	–	–	–	0.46	–

by the land breezes channeled along the Llobregat River, which delimits the western side of Barcelona (Dall'Osto et al., 2012). By contrast, Ni was observed both in the night and in the afternoon when sea breeze brings pollution from the port, as reported in previous studies (Moreno et al., 2011). Finally, Zn was found to possess a complex diurnal profiles likely due to a combination of traffic and industrial sources.

### 3.1.4 Air mass influences

Average concentrations as a function of different air mass for both sites were investigated, in order to see the effect of air masses on the selected elements. Back trajectories of the air masses arriving at Barcelona were calculated for each day of the campaign, depicting the path taken by the air mass reaching the sampling site over the previous five days by using the on-line HYSPLIT model. A detailed description is found in the presenting overview of this ACP special issue (Dall'Osto et al., 2012). Some elements presented more than a 2-fold concentration increase at both sites (relative to average concentration) under specific air masses: Al, Ti, K and Fe under North African East air masses (NAF\_E, air masses originated in the Saharan region arriving from the Easterly sector). By contrast, Zn, Pb, Mn, Cl concentrations were found enhanced under Northerly Atlantic air masses (ATL, intensive cold advections from the Atlantic Ocean). Other elements did not show any clear trends. In summary, the complex spatial and temporal relationship of the elements measured in this study did reveal some interesting pattern, but it was not able to sensibly advance our understanding of the aerosol sources identification. For this reason, receptor modelling was applied on the hourly concentrations of the elements measured and the results are presented in the next section.

## 3.2 PMF analysis results

Rotational ambiguity and validness of the proposed solution were explored by analysing different FPEAK rotations (0.0 resulted the most realistic solution), several seeds, distribution of scaled residuals and Q/Q<sub>exp</sub> ratio. Nine factors were identified as the best solution, also supported by correlation with external data (Aerosol Time-of-Flight Mass Spectrometry – ATOFMS).

### 3.2.1 Identification of the PM<sub>2.5</sub> sources

The nine factors obtained are reported in Fig. 4: the average source contributions to the elemental concentrations ( $\text{ng m}^{-3}$ , left y-axes, blue columns) and percentages (% , right y-axes, red squares). Three groups were identified, associated to regional sources (regional sulphate, sea salt and biomass burning), spikes of anthropogenic activities (industrial emissions and oil combustion) and three types of dust (non-exhaust primary traffic brake dust, soil dust and urban dust).

- *Regional sulphate: Reg. (S), Fig. 4a, (percentage of total element mass detected: RS 26 %, UB 29 %).* This source is characterised by Sulphur and it is likely due to the regional background contribution of sulphates, mainly in the form of ammonium sulphate. This component is attributed to secondary sulphate and aged aerosols, it explains the highest fraction of S mass concentrations (64 %).
- *Sea-salt: S.S. (Na-Mg), Fig. 4b, (RS 18 %, UB 15 %).* Primarily characterised by Na and Mg, the Mg/Na suggests that these two elements originate from the same

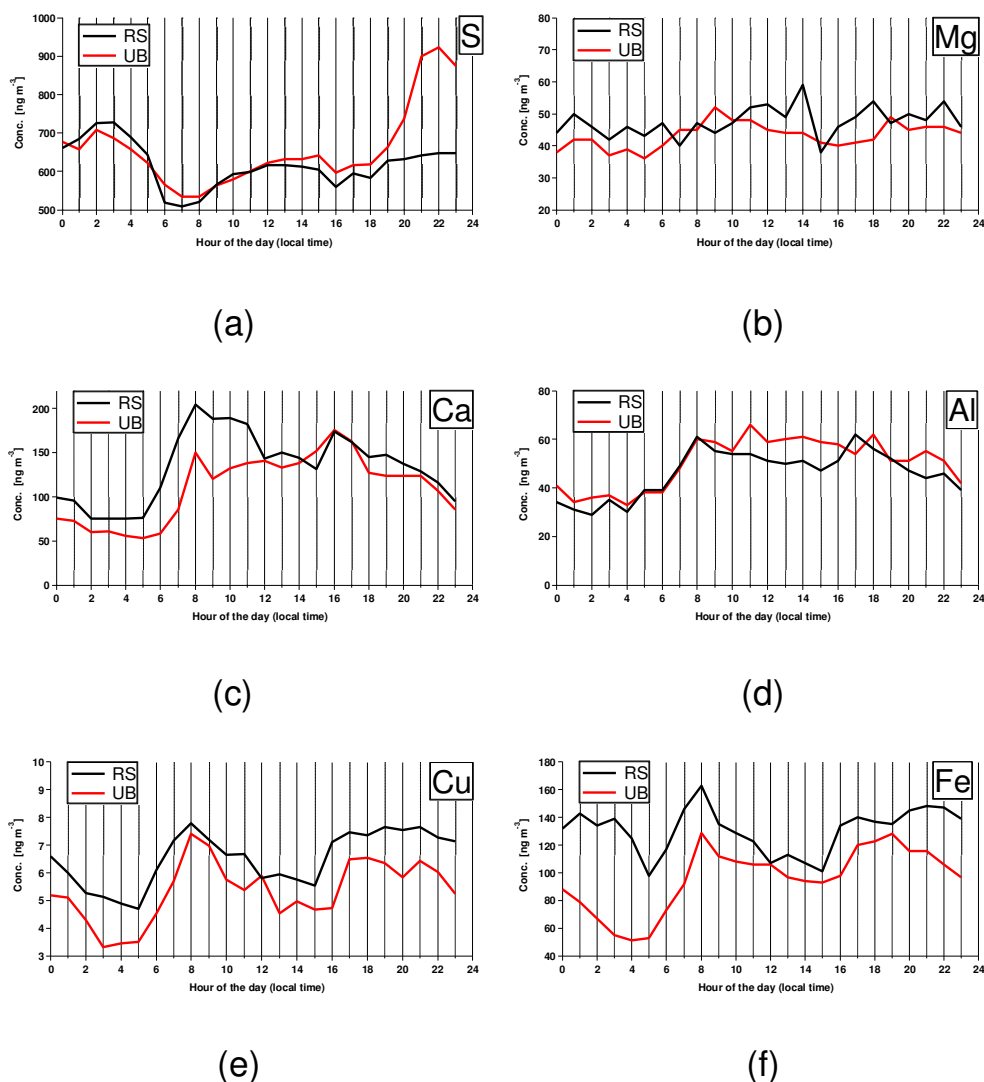


**Fig. 3.** Diurnal profile of selected elements at the UB and RS site.

source and have a marine origin. The lack of Cl in this source indicates that a large fraction of the Cl was depleted. Most of Na (59 %) and Mg (41 %) mass concentrations are described by this factor.

- *Biomass burning: B.B. (K)*, Fig. 4c, (RS 4 %, UB 6 %). This source is characterised by K (56 % of total detected K signal), with small contribution of Cu. The enhancement of Cu and Pb was previously reported in previous studies, likely to be due to anthropogenic contaminants burned along with open log-wood fires (Nriagu and Pacyna, 1988; Karanasiou et al., 2009; Richard et al., 2011).
- *Soil dust (Al-Ti)*, Fig. 4d, (RS 11 %, UB 13 %). This source is characterised by Al and Ti with contributions from other crustal elements (K, Ti, Ca, Fe and Mn) as well as Na and Mg. This factor described 68 %,

43 % and 24 % of Al, Ti and Fe, respectively. An increase of this factor was found to occur under North African Tropical air masses and attributed to Saharan dust (Dall'Osto et al., 2012), with average concentrations of  $550 \pm 200 \text{ ng m}^{-3}$  (max values:  $1800 \text{ ng m}^{-3}$ ). However, it is important to note that this factor was also detected as background concentrations before and after the Saharan dust events, although with much lower concentrations ( $110 \pm 65 \text{ ng m}^{-3}$ , max values  $393 \text{ ng m}^{-3}$ ).

- *Urban Dust (Ca)*, Fig. 4e, (RS 7 %, UB 6 %). This profile is characterised primarily by Ca, and, to a lesser extent, by Al, K, Ti and Mn. Because of its composition, this source is related to crustal urban soil dust. This PMF factor describes 65 % of the calcium concentrations detected during SAPUSS. The urban dust factor found in this study can be due not only to soil



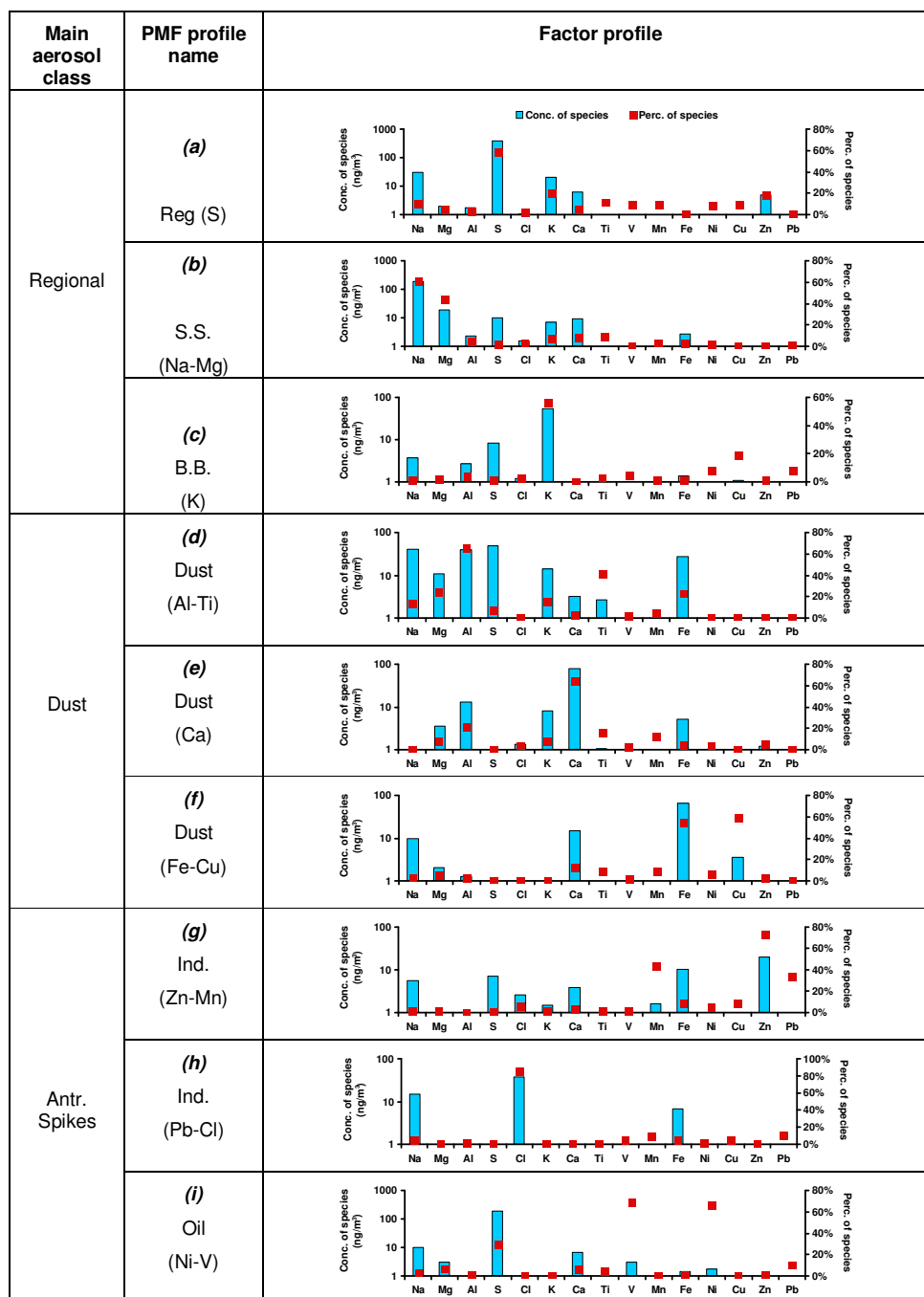


Fig. 4. PMF factor factors.

but also to other anthropogenic activities such as construction, demolition works and releases from buildings and other surfaces through weathering and other erosive processes. The most important construction-related activities in term of their contribution to particulate matter concentrations are earth-moving operations (Muleski et al., 2005). Barmpadimos et al. (2011) reported very high contribution of traffic coarse mode urban ambi-

ent concentrations, but it was stressed that these numbers are somewhat overestimating the traffic contribution because of the lack of information on construction activities around the considered sites. Scarce precipitation limits the cleansing of paved surfaces and, as a result, re-suspension is favoured. Further consideration on the effect of precipitation on this source is given in Sect. 4.2.

– *Brake dust (Fe-Cu)*, Fig. 4g, (RS 9%, UB 5%). This profile is characterised by Fe and Cu (53% and 60% of the total concentrations monitored, respectively). These elements are typical traffic markers, as the abrasion of brakes produces particles characterised by high concentrations of Cu, Ba, Zn and Fe (Sanders et al., 2003; Johansson et al., 2008).

This aerosol source was found the only one of this study correlating well ( $R^2=0.7$ ) with Black Carbon (BC), suggesting that this primary non-exhaust traffic brake dust source is co-emitted along with the primary exhaust traffic BC one. Another source of primary traffic non-exhaust aerosols are particles released by mechanical abrasion of tyres which are characterised by high concentration of Zn (Johansson et al., 2008). In a previous work in Barcelona, Amato et al. (2011) did not show a roadside enrichment for fine aerosol Zn concentrations, but suggested that 15% of coarse Zn may be attributed to road traffic emissions. This dust (Fe-Cu) profile only explained about 5% of the Zn variation, and a specific PMF factor related to tyre dust was not found in this study.

– *Industrial (Zn-Mn)*, Fig. 4g, (RS 3%, UB 4%). This profile is attributed to an industrial source characterised by Zn, Mn and some Pb. These metals were previously attributed to emissions from smelters (Moreno et al., 2011). Amato et al. (2010) also reported a PMF factor with high concentrations of Zn, Pb and Mn and attributed it to industrial emissions, whereas a similar factor was attributed more to local workshops and ateliers in the city of Zurich (Richard et al., 2011).

– *Industrial (Pb-Cl)*, Fig. 4h, (RS 8%, UB 3%). This factor is a second type of industrial aerosol emissions characterised by Cl, Pb and some Mn. It is important to note that 82% of the Chlorine detected during SAPUSS is described by this PMF factor. Whilst this source was never reported in previous works in this region (Moreno et al., 2011; Amato et al., 2010, 2011), its validity is supported by striking external correlation with hourly measurements taken by aerosol time-of-flight mass spectrometry measurements (ATOFMS, Fig. 5a). It is essential to use correlations between the obtained PMF factor time series and external measurements time series in order to support the validity of the PMF solution presented. Figure 5b shows the positive and negative mass spectra of a particle type detected at both monitoring sites with the ATOFMS (Dall'Osto et al., 2012). Pb was found to be one of the largest contributors to the positive ion spectrum occurring at  $m/z$  +206, +207 and +208. Often internally mixed with Pb, Zn ions appear at  $m/z$  +64. Other peaks in the positive ion spectrum include  $m/z$  23 (Na),  $m/z$  56 (Fe),  $m/z$  39 and 113 (K and  $K_2Cl$ ). In addition to nitrate ( $m/z$  -46  $NO_2$  and

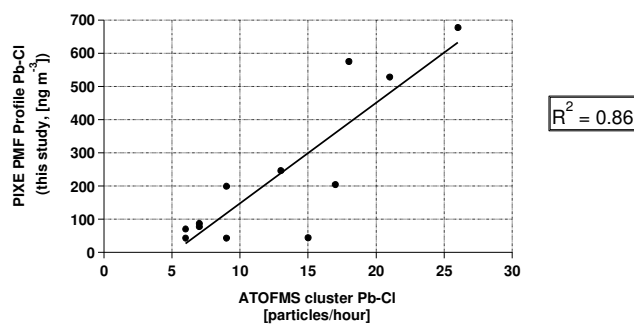


**Fig. 5a.** Temporal hourly correlation between the PMF factor profile Ind. (Pb-Cl) and an ATOFMS particle type (Pb-Cl), see Dall'Osto et al. (2012).

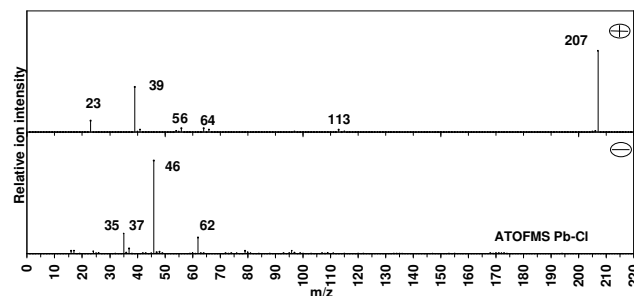


**Fig. 5b.** Average positive and negative mass spectra of particle type Pb-Cl detected at the RS site by single particle aerosol mass spectrometry (ATOFMS).

$m/z$  -62  $NO_3$ ), chloride ( $m/z$  -35 Cl) is one of the most abundant ion in the negative spectra. In general, zinc and lead chlorides have relatively low boiling points and are emitted in the gas phase of high temperature combustion sources such as waste incinerators (Hu et al., 2003). Combustion of municipal waste produces submicron particles composed of Zn and Pb as well as numerous other metals, and relative to nonferrous smelters, such aerosol emissions are enriched in Cl (Tan et al., 2002). A similar Pb-Cl ATOFMS particle type detected during SAPUSS (Fig. 5a, b) was previously associated to a waste incinerator source (Moffet et al., 2008a, b) although other studies in the same area (Mexico city) attributed it to multiple sources, including trash burning (Salcedo et al., 2010; Hodzic et al., 2012). Earlier metallurgical source studies also showed high  $SO_2$  concentrations with Pb-Zn smelter plumes, but our study is in line with the one of Moffet et al. (2008a, b) showing weak correlations observed between this aerosol source and  $SO_2$ .

– *Oil combustion (Ni-V)*, Fig. 4i, (RS 13%, UB 17%). This source is characterised by elements like V or Ni, tracers for any combustion process of heavy oils (Pacyna and Pacyna, 2001). This source may, therefore, be

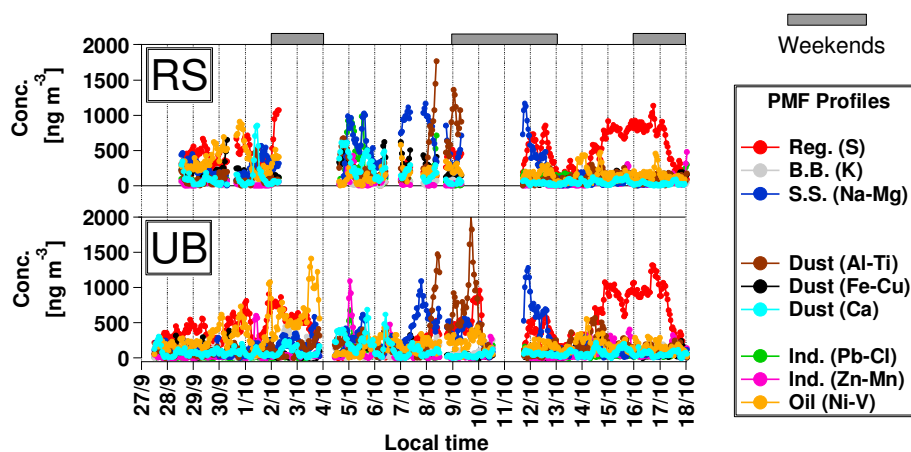


Fig. 6. Temporal trends of the nine PMF factors detected simultaneously at the UB and RS site.

**Table 3.** Percentages (% , sum of the masses of the elements analysed) of the nine PMF factors at the UB, RS and average UB-RS (MEAN) sites.

Class	PMF factor name	MEAN (UB-RS)	UB	RS
Regional	Reg. (S)	27 %	29 %	26 %
	S.S. (Na-Mg)	17 %	15 %	18 %
	B.B. (K)	5 %	6 %	4 %
Dust	Dust (Fe-Cu)	7 %	5 %	9 %
	Dust (Ca)	6 %	6 %	7 %
	Dust (Al-Ti)	12 %	13 %	11 %
Plumes	Ind. (Pb-Cl)	5 %	3 %	8 %
	Ind. (Zn-Mn)	3 %	4 %	3 %
	Oil (Ni-V)	15 %	17 %	13 %
TOTAL		100 %	100 %	100 %

due both to the activities of the port and the industrial areas of the Barcelona urban area. This profile was found the only one of the nine herein reported correlating with  $\text{SO}_2$ .

In summary, the nine PMF factors presented give a much better interpretation of the results respect to what can be obtained by only looking at correlations among elements (Sect. 3.1). PMF was able to separate regional and local sources, and further results on abundance, temporal trends, diurnal profiles and site inter comparison of PMF factors are given in the next sections.

### 3.2.2 Abundance, temporal trends, diurnal patterns and site intercomparison of the PMF factors

Table 3 shows the percentage of the  $\text{PM}_{2.5}$  elemental mass (sum of all detected elements) of the nine factors at the two different monitoring sites (UB, RS) as well as the average of the two (MEAN). The frequency mass concentrations distributions of the hourly data are presented in Fig. S2. The three regional factors (Reg. (S), S.S. (Na-Mg) and B.B. (K)) did

not present much variation between the sites, and overall represented 56 % of the aerosol mass detected by the PIXE. By contrast, some factors were enhanced at the RS site (Brake dust (Fe-Cu) and Ind. (Pb-Cl)), whereas higher proportion of Oil (Ni-V) were found at the UB site (Table 3). PMF modelling from daily  $\text{PM}_{2.5}$  in other WMB sites also identified similar sources but traffic related dust was found mixed with secondary and non-exhaust ones, likely due to the low time resolution used, hence, the impossibility to separate multiple sources (Oliveira et al., 2010). Figure 6 shows the temporal trends of the nine different sources apportioned at both sites. A number of different periods can be seen, including a Saharan dust intrusion (8–10 October) and a regional accumulation one (14–17 October). When the factors are apportioned to different air masses (Dall'Osto et al., 2012), Table 4 shows – as expected – that Reg. (S) has a higher impact under regional air masses scenarios (42 %), and the least ones under the Atlantic air masses scenarios (17 %). The highest loading of soil dust is under NAF air masses from the East sector (37 %). By contrast NAF West air masses (only one day, 3 October) characterised by strong wind coming from the port areas (230–270°) apportion up to 45 % to Ind. (Ni-V) source. Finally, it is interesting to note that Urban dust (Ca) showed the highest percentages under windy Atlantic air mass scenarios (Table 4) favouring resuspension.

The validity of the PMF solution is also supported by the correlations shown in Table 5 among the two different sites. Whilst elements concentrations among sites (Sect. 3.1, Table 2) were not found highly correlated, our receptor modelling study is able to separate local from regional sources quite well. The correlation between Reg. (S) among sites for example is very high ( $R^2 = 0.88$ ). Other regional sources also show good correlations among the two monitoring sites: Soil dust (Al-Ti) ( $R^2 = 0.69$ ) and S.S. (Na-Mg) ( $R^2 = 0.55$ ). By contrast, the Brake dust (Fe-Cu) does not appear correlated with any other source, due to its local traffic nature. Industrial sources showed weaker correlations among

**Table 4.** Abundance of the PIXE total mass (%) of the nine PMF factors for different air mass scenarios.

	Reg. (S)	Ind (Pb-Cl)	Dust (Fe-Cu)	B.B. (K)	Ind (Zn-Mn)	S.S. (Na-Mg)	Dust (Al-Ti)	Oil (V-Ni)	Dust (Ca)
Regional (REG)	42	5	8	6	4	7	8	16	4
Atlantic (ATL)	17	10	9	3	5	21	8	14	11
North African East (NAF_E)	19	2	4	3	0	22	37	10	3
North African West (NAF_W)	23	0	1	5	1	11	11	45	3

the sites, perhaps due to a number of reasons including RS street canyon characteristics and dimension of aerosol industrial aerosols plumes.

Finally, the diurnal trends of the aerosol sources profiles are presented in Fig. 7 for both sites. Whilst there was not a clear diurnal variation for the regional aerosol sources profile (Fig. 7a–c), the soil dust (Al-Ti) was mainly detected in the morning during the Saharan dust outbreak (Fig. 7d). The brake dust (Fe-Cu) source shows two peaks coinciding with rush hours, with the morning one at 8 a.m. far more pronounced (Fig. 7e). The time trend of this source is well correlated with the vehicles traffic count profile ( $R^2 > 0.7$  at both sites). Interesting is the behaviour of the urban dust source (Dust (Ca), Fig. 7f), which was not found correlating with vehicles traffic counts. The rise in the concentrations at both sites is at morning traffic rush hours, but the concentrations remain high during the day with a pronounced increase in the late afternoon. This implies that whilst brake dust (Fe-Cu) is related to primary aerosols coming from non-exhaust particles directly emitted by vehicles, the elements (mainly Ca) in the urban soil source are composed by re-suspended road dust and soil transported by wind (maximum at 3 p.m. at the UB due to the sea breeze) and/or re-suspended by human activities. Re-suspension of dust is function of a number of complex variables such as wind speed, number of cars and speed of cars. Moreover, in street canyon speed of cars may create a vortex which may be more effective in re-suspension. Amato et al. (2010) also found a comparable mineral factor with constantly higher concentrations during the day without significant variation within the daylight hours of the day.

Oil combustion (Ni-V) presented a minimum in the middle of the day and maxim during the night, pointing to a main contribution from the industrial area, but also from the port areas (Fig. 7g). Finally, the two industrial factors presented complex diurnal profiles (Fig. 7h–i), with aerosol plumes impacting the city during both day and night time.

### 3.2.3 Comparative demonstration of different PMF solutions

The solution presented above is the best of the ones investigated in this study. It represents at an hourly resolution nine different aerosol sources detected simultaneously at two different monitoring sites. A lower ( $< 9$ ) number of PMF fac-

tors did not explain well all the aerosol sources, whereas a higher ( $> 9$ ) number created splitting of PMF factors. The solution presented in Sect. 3.2 was also found better than other ones using different datasets, including:

- Daily resolution data. The hourly data were merged to daily bins, and the PMF was run on the 24 h samples. The interpretation of the results was less clear and the association of the obtained PMF factors to specific aerosol sources really challenging. In particular, the industrial and shipping oil emissions (V-Ni) and the dust profiles (Fe-Cu) were all merged in broad undefined PMF factors.
- Hourly PIXE dataset without days of 8, 9, 10 October (Saharan dust event). Only one broad crustal dust aerosol source was found (mainly Al, Ti, Ca, Fe). Moreover, oil emissions (V) were found mixed with aerosol dust sources (Fe-Cu).

## 4 Discussion and conclusion

### 4.1 Intercomparison between ATOFMSs results and hourly PMF PIXE factors

The ATOFMS provides information on the abundance of different organic and inorganic types of aerosol particles as a function of size with high time resolution at single particle level. ATOFMS can also provide quantitative chemical information if a relative sensitivity factor is applied (Dall'Osto et al., 2006). Two ATOFMS were deployed simultaneously during the SAPUSS field study at the RS (TSI 3800-100, aerodynamic lens) and at the UB (TSI 3800, nozzle/skimmer), respectively. During the SAPUSS, 18 and 14 different particle types were apportioned at the RS and at the UB, respectively, 10 of which were found the same at both sites. Most of the particle types were found rich in organic carbon, elemental carbon and nitrate (Dall'Osto et al., 2012). Giving the fact that the PIXE technique is able to detect only selected elements, a complete intercomparison of the two techniques is not straight forward. Most of the PMF factors obtained from this study did not present significant correlations with the ATOFMS particle types. However, fairly good correlations were obtained with the three regional PIXE PMF factors (Reg. (S) correlating  $R^2 = 0.85$  with ATOFMS regional

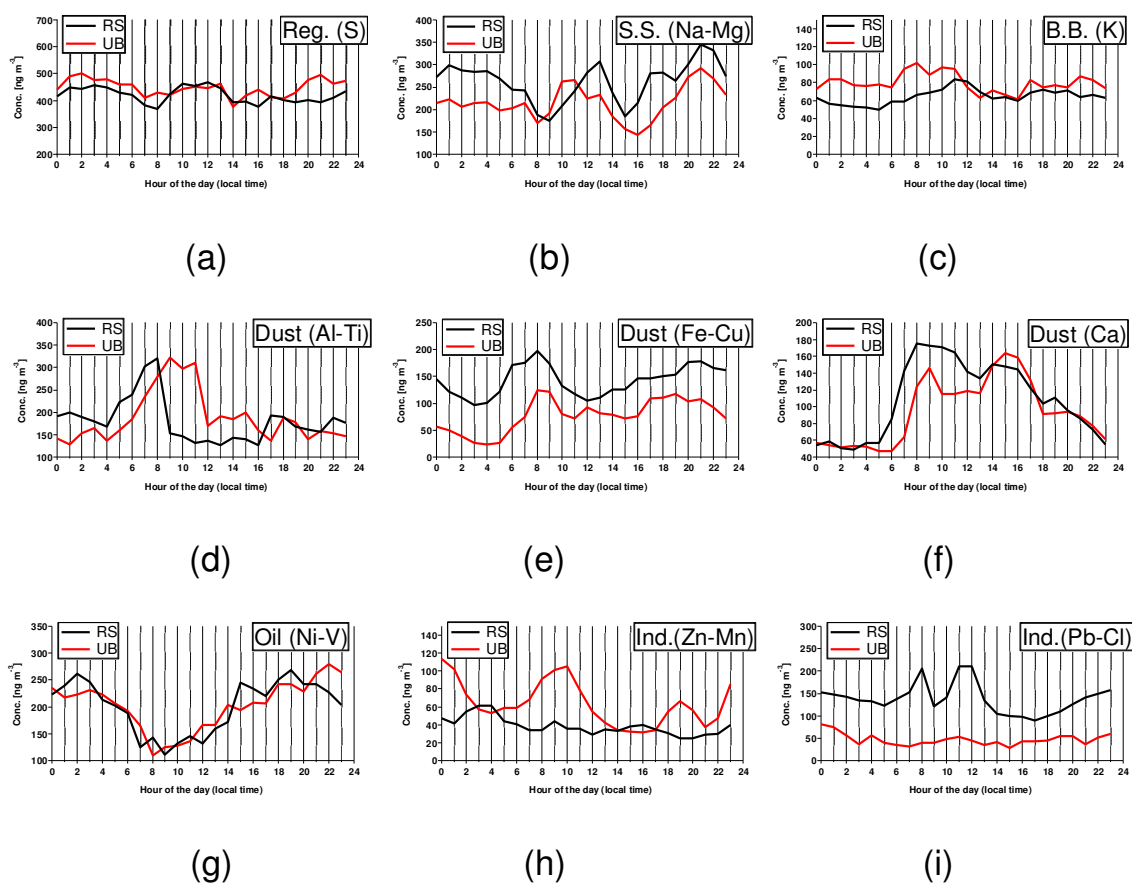


Fig. 7. Diurnal profile of the PMF factors at the UB and RS site.

aged EC; B.B. (K) correlating  $R^2=0.45$  with ATOFMS K-CN and S.S. (Na-K) correlating  $R^2=0.35$  with ATOFMS NaCl) at both monitoring sites. Specific ATOFMS particle types detected only at the UB site were found correlating with the PMF PIXE factors: ATOFMS V-rich shipping oil combustion with PIXE PMF Oil (Ni-V) –  $R^2=0.55$  – and ATOFMS dust with PIXE PMF dust (Al-Ti) –  $R^2=0.65$ . Overall, the strongest correlation ( $R^2=0.86$ ) was found to be between ATOFMS Pb-Cl and PIXE Ind. (Pb-Cl), as already discussed in Sect. 3.1 and Fig. 5.

It is important to note that hourly temporal trends of selected metals can be obtained by querying specific  $m/z$  ratios in the ATOFMS dataset. Within this SAPUSS special issue, hourly integrated ATOFMS peak areas of selected  $m/z$  ratios will be evaluated for their suitability in representing metals by comparing them with the metals concentrations presented in this study.

## 4.2 Air quality considerations from the PMF PIXE sources

### 4.2.1 Regional particle types

Secondary sulphate (Reg. (S)), which is present in secondary and aged aerosol, explains the highest fraction (RS: 26 %, UB: 29 %) of elemental mass concentration in the fine PM. This factor does not exhibit a clear diurnal variation, indicating a regional rather than a local source. Amongst the sources most difficult to quantify by receptor modelling, and for which emissions inventory data are least reliable, wood smoke stands out as posing particular problems (Harrison et al., 2012). Our receptor modelling study was able to separate a factor which we attribute to biomass burning mainly of regional origin. Interestingly, the main regional contribution of the B.B. (K) factor is further supported by its correlation with the Reg. (S) profile (Table 5). These two factors were found the only ones to be both inter- and intra-related within the two monitoring sites. However, a stronger correlation between Reg. (S) and B.B. (K) was found at the RS ( $R^2=0.52$ ) than at the UB site ( $R^2=0.27$ ). The reason may be due to additional local biomass burning (residential stoves) partially impacting the UB site.

**Table 5.** Correlation Table ( $R^2$  of the nine PMF profile simultaneously detected at the UB and RS site. Poor correlations ( $R^2 < 0.25$ ) are not reported for clarity (-).

		RS								
		Reg (S)	Ind (Pb-Cl)	Dust (Fe-Cu)	B.B. (K)	Ind (Zn-Mn)	S.S. (Na-Mg)	Dust (Al-Ti)	Oil (Ni-V)	Dust (Ca)
UB	Reg (S)	0.88	-	-	0.52	-	-	-	-	-
	Ind (Pb-Cl)	-	0.51	-	-	-	-	-	-	-
	Traf (Fe-Cu)	-	-	-	-	-	-	-	-	-
	B.B. (K)	0.27	-	-	0.35	-	-	-	-	-
	Ind (Zn-Mn)	-	0.27	-	-	0.25	-	-	-	-
	S.S. (Na-Mg)	-	-	-	-	-	0.55	-	-	-
	Dust (Al-Ti)	-	-	-	-	-	-	0.69	-	-
	Oil (Ni-V)	-	-	-	-	-	-	-	0.37	-
	Dust (Ca)	-	-	-	-	-	-	-	-	0.39

As regards to sea spray, the factor we identified (S.S. (Na-Mg); RS:18 % UB: 15 %) suggested a strong depletion in Cl. The weak presence of S in this factor confirms the ATOFMS studies showing that the sea spray detected during SAPUSS was mainly internally mixed with nitrate and not with sulphate (Dall'Osto et al., 2012). In summary, we find a similar impact of regional aerosol sources on both sites in spite of the fact that the UB site is far more ventilated than the RS one.

#### 4.2.2 Dust

In urban environments coarse  $PM_{10}$  particles tend to be dominated by non-exhaust traffic particles including brake dust and resuspension and wind-blown soil. Amato et al. (2009) showed that soil (mineral) and brake (road) dust can also apportion 12 % and 8 % (respectively) of the finer  $PM_{2.5}$  monitored in the city of Barcelona. The present study was successful at separating different types of dust, attributed to three different sources and altogether representing 25 % of the elements mass concentrations measured. The temporal trends of soil dust (Al-Ti) particles clearly pointed to a strong Saharan Desert origin, as they were mainly detected during the period of 8–10 October under North African air mass scenarios (Dall'Osto et al., 2012). However, this particle type was also detected at lower background concentrations during other periods of the SAPUSS field study (Fig. 6). By contrast, the occurrence of urban Dust (Ca) presented a more local origin. Substantial source of aerosol particles from the road traffic is also the mechanical abrasion of the pavement. These

particles typically contain high concentrations of Si, Al, Ca, Mg and Fe (Sternbeck et al., 2002). During this study, we were not able to find a specific PMF factor for the mechanical abrasion of the pavement, likely to be mixed within the three different dust types. However, we found a specific brake dust (Fe-Cu) type which we attribute to non-exhaust primary vehicles emissions. Street geometry and atmospheric circulations can affect the  $PM_{10}$  roadside concentrations (Harrison et al., 2004), although previous street canyon studies in Barcelona did not reveal clear wind speed dependence (Amato et al., 2011). A great effort was made in understanding the relationship between wind components, traffic counts and the  $PM_{2.5}$  aerosol mass concentrations of the three different dust particles. Unfortunately, the only correlation found was the obvious reduction (dilution) of concentrations at higher wind speed for all three dust particle types. The reasons of the complex relationships between wind components, traffic counts and the dust particles may be due to the finer fraction analysed ( $PM_{2.5}$ , more dependent to dilution processes rather than resuspension ones as opposed to the coarser  $PM_{10}$  fraction.)

Interestingly, we did not find uniform variations for different dust particle types under rainy conditions. Two time periods were identified as dry days (4, 5, 6 October, DD, average rain amount:  $0.0 \text{ mm h}^{-1}$ ) and rainy days (11, 12, 13 October, RD, average rain amount:  $0.25 \text{ mm h}^{-1}$ ). Wet days (relative to dry days) were found colder ( $17^\circ\text{C}$  vs.  $21^\circ\text{C}$ ), windier ( $4.3 \text{ m s}^{-1}$  vs.  $2.4 \text{ m s}^{-1}$ ), cloudier ( $89 \text{ W m}^{-2}$  vs.  $189 \text{ W m}^{-2}$ ) and with higher RH (75 % vs. 58 %). Average hourly concentrations were calculated for a number of

chemical species for the two different periods. A DD/RD ratio of  $1.5 \pm 0.5$  (1–2) was found for primary aerosols (BC) and the six non-dust PIXE PMF factors (Reg. S, B.B. K, S.S. Na-Mg, Ind. Zn-Mg, Ind. Pb-Cl, Oil Ni-V). By contrast, a ratio of 3, 4 and 8 was found for the soil dust (Al-Ti), brake dust (Fe-Cu) and urban dust (Ca), respectively. In other words – as expected – resuspended urban dust (Ca) is the particle type most affected by the wetness of the land. This effect is likely to be due to both rain wash and/or road wetting, hence, limiting resuspension.

#### 4.2.3 Anthropogenic industrial plumes and urban chlorine aerosol sources.

The Iberian Peninsula presents several industrial activities related to refuse incineration and metallurgy. During SAPUSS, three types of anthropogenic industrial plumes apportioned 23 % of the PIXE elemental mass concentrations. We found a particle type typical of oil combustion sources (Oil (Ni-V)), correlating with SO<sub>2</sub>, attributed to shipping oil combustions and already reported in previous studies (Viana et al., 2006; Amato et al., 2010). Another common source found was rich in Zn and Mn (Ind. (Zn-Mn)) and previously attributed to smelters (Viana et al., 2006).

However, a unique particle type was reported for the first time in the Barcelona area, called Ind. (Pb-Cl) and associated with a combustion source. Municipal and hazardous waste incinerator have been shown to emit Pb, Zn and Cl particles (Walsh et al. 2001; Tan et al., 2002; Hu et al., 2003). For this source, Cl is primarily from the burning of plastic such as polyvinyl chloride and paper, whereas the Pb and Zn can be produced from a variety of sources. We systematically found higher concentrations of aerosol associated with Ind. (Zn-Ni) at the UB site relative to the RS ones, whereas the opposite trend was found for the Ind. (Pb-Cl) source. Dall'Osto et al. (2012) reported a detailed analysis of the gaseous concentrations at all different SAPUSS monitoring sites. It was found that the diurnal profile of CO shows a similar trend of NO for most of the monitoring sites, confirming its main traffic source. However, an additional CO spike at 1 pm (not associated with NO) was evident only at the RS diurnal cycle, pointing out to a non-vehicular combustion localised source.

During night times the two industrial sources (Zn-Mn and Pb-Cl) were often correlated at both monitoring sites, hence, likely to be associated with smelters activities. By contrast, the spike of Ind. (Pb-Cl) seen at 1 pm (not seen for the Ind. Zn-Mn source) at the RS site points out to a local urban combustion source.

On that regard, some considerations should be made on fine particle antimony (Sb), recently suggested as garbage burning tracer (Christian et al., 2010) although Sb is also used as a main tracer of vehicle brake emissions in cities (Sternbeck et al., 2002; Querol et al., 2008; Hodzic et al., 2012). During our study we did not find a clear association of Sb (obtained by ICP-MS/ICP-AES analysis, Dall'Osto et al.,

2012) with this Ind. (Pb-Cl) source. Finally, Li et al. (2012) reported up to 3 ppb HCl in Mexico city, suggesting garbage burning as a major (up to 60 %) source of particulate Chloride. Our study also suggests that Pb-Cl combustion emissions are a major source of fine Cl in the city centre of Barcelona, with maximum concentrations up to  $530 \text{ nm m}^{-3}$ .

#### 4.3 Conclusion

Hourly-resolved elemental concentration data obtained by the combined use of streaker samples followed by PIXE analysis were successfully used to determine both the source origin of aerosol PM<sub>2.5</sub> elemental mass in urban environments and their contribution to the concentrations of the detected elements. The concentrations of the elements depend on a complex interplay of factors that include local geomorphology, meteorological variations, patterns of road use and specific contributions from industrial hotspots. The detailed chemical database with high time resolution presented in this paper demonstrates in more detail than previous studies that the spatial and temporal variability of atmospheric element content is a likely characteristic of Barcelona urban area and offers a deeper insight in source identification. By using PMF analysis, we find a number of local as well as regional sources and natural as well as anthropogenic sources. On a total elemental mass basis (17 detected elements), the most important isolated factor was found to be associated with secondary sulphate (27 %). This was followed by sea salt (17 %) and shipping oil combustion (15 %). Three types of dust particles were found originating from traffic brake dust, urban mineral dust, soil dust and representing 25 % of the total mass detected. This study confirms that aerosol dust is an important source of PM in urban areas in southern Europe (Putaud et al., 2010). A clear advantage of the high time resolution is the possibility to enable the identifications of sources varying at different hours of the day. This is particularly important for aerosol sources that are more locals (spikes events lasting only few hours) rather than regional contributions (lasting longer periods as more influenced by long-range transport or air mass back trajectories type). Quantitative results from this study were also correlated with qualitative single particle mass spectrometry measurements. Overall, the PMF receptor modelling applied to the hourly resolution elemental concentrations obtained by PIXE has proven useful in separating different regional aerosol sources, different types of dusts, and different types of industrial plume-like events during the SAPUSS project.

**Supplementary material related to this article is available online at: <http://www.atmos-chem-phys.net/13/4375/2013/acp-13-4375-2013-supplement.pdf>.**

**Acknowledgements.** FP7-PEOPLE-2009-IEF, Project number 254773, SAPUSS – Solving Aerosol Problems Using Synergistic Strategies (Marie Curie Actions – Intra European Fellowships. Manuel Dall'Osto). This study was also supported by research projects from the D. G. de Calidad y Evaluacion Ambiental (Spanish Ministry of the Environment) and the Plan Nacional de I+D (Spanish Ministry of Science and Innovation [CGL2010-19464 (VAMOS) and CSD2007-00067 (GRACCIE)]), the Spanish Agency for Management of University and Research Grants (AGAUR), a collaboration agreement CSIC-JRC, and the Departaments de Medi Ambient from the Generalitat de Catalunya and Diputacio de Barcelona. The University of Birmingham (UK) and the University of Cork (Ireland) SAPUSS ATOFMS teams are also acknowledged.

Edited by: R. M. Harrison

## References

- Amato, F., Pandolfi, M., Escrig, A., Querol, X., Alastuey, A., Pey, J., Perez, N., and Hopke, P. K.: Quantifying road dust resuspension in urban environment by Multilinear Engine: A comparison with PMF2, *Atmos. Environ.*, 43, 2770–2780, 2009.
- Amato F., Nava S., Lucarelli F., Querol X., Alastuey A., Baldasano J. M., and Pandolfi, M. A: Comprehensive assessment of PM emissions from paved roads: Real-world Emission Factors and intense street cleaning trials, *Sci. Total Environ.*, 408, 4309–4318, 2010.
- Amato, F., Viana, M., Richard, A., Furger, M., Prévôt, A. S. H., Nava, S., Lucarelli, F., Bukowiecki, N., Alastuey, A., Reche, C., Moreno, T., Pandolfi, M., Pey, J., and Querol, X.: Size and time-resolved roadside enrichment of atmospheric particulate pollutants, *Atmos. Chem. Phys.*, 11, 2917–2931, doi:10.5194/acp-11-2917-2011, 2011
- Barnpadimos, I., Nufer, M., Oderbolz, D. C., Keller, J., Aksoyoglu, S., Hueglin, C., Baltensperger, U., and Prévôt, A. S. H.: The weekly cycle of ambient concentrations and traffic emissions of coarse (PM<sub>10</sub>–PM<sub>2.5</sub>) atmospheric particles, *Atmos. Environ.*, 45, 4580–4590, doi:10.1016/j.atmosenv.2011.05.068, 2011.
- Brunekreef, B. and Holgate, S. T.: Air pollution and health, *Lancet*, 360, 1233–1242, 2002.
- Brunekreef, B. and Forsberg, B.: Epidemiological evidence of effects of coarse airborne particles on health, *Europ. Respir. J.*, 26, 309–318, 2005
- Calzolari G., Chiari, M., Garcia Orellana, I., Lucarelli, F., Migliori, A., Nava, S., and Taccetti, F.: The new external beam facility for environmental studies at the Tandemron accelerator of LABE C, *Nucl. Instrum. Meth. B*, 249, 928–931, 2006.
- Chiari, M., Lucarelli, F., Mazzei, F., Nava, S., Paperetti, L., Prati, P., Valli, G., and Vecchi, R.: Characterization of airborne particulate matter in an industrial district near Florence by PIXE and PESA, *X-Ray Spectrom.*, 34, 4, 323–329, 2005.
- Christian, T. J., Yokelson, R. J., Cárdenas, B., Molina, L. T., Engling, G., and Hsu, S.-C.: Trace gas and particle emissions from domestic and industrial biofuel use and garbage burning in central Mexico, *Atmos. Chem. Phys.*, 10, 565–584, doi:10.5194/acp-10-565-2010, 2010.
- Dall'Osto, M., Harrison, R. M., Beddows, D. C. S., Freney, E. J., Heal, M. R., and Donovan, R. J.: Single particle detection efficiencies of aerosol time of flight mass spectrometry during the North Atlantic marine boundary layer experiment, *Environ. Sci. Technol.*, 40, 5029–5035, doi:10.1021/es050951i, 2006
- Dall'Osto, M., Querol, X., Alastuey, A., Minguillon, M. C., Alier, M., Amato, F., Brines, M., Cusak, M., Grimalt, J. O., Karanasiou, A., Moreno, T., Pandolfi, M., Pey, J., Reche, C., Ripoll, A., Tauler, R., Van Drooge, B. L., Viana, M., Harrison, R. M., Gietl, J., Beddows, D., Bloss, W., O'Dowd, C., Ceburnis, D., Martucci, G., Ng, S., Worsnop, D., Wenger, J., Mc Gillcuddy, E., Sudou, J., Healy, R., Lucarelli, F., Nava, S., Jimenez, J. L., Gomez Moreno, F., Artinano, B., Prevot, A. S. H., Pfaffenberger, L., Frey, S., Wilsenack, F., Casabona, D., Jimenez-Guerrero, P., Gross, D., and Cotz, N.: Presenting SAPUSS: solving aerosol problem by using synergistic strategies at Barcelona, Spain, *Atmos. Chem. Phys. Discuss.*, 12, 18741–18815, doi:10.5194/acpd-12-18741-2012, 2012.
- Denier van der Gon, H. A. C., Hulskotte, J. H. J., Visschedijk, A. J. H., and Schaap, M.: A revised estimate of copper emissions from road transport in UNECE-Europe and its impact on predicted copper concentrations, *Atmos. Environ.*, 41, 8697–8710, 2007.
- De la Campa, A. M. S., de la Rosa, J., Gonzalez-Castanedo, Y., Fernandez-Camacho, R., Alastuey, A., Querol, X., Stein, A. F., Ramos, J. L., Rodriguez, S., Orellana, I. G., and Nava, S.: Levels and chemical composition of PM in a city near a large Cu-smelter in Spain, *J. Environ. Monitor.*, 13, 1276–1287, 2011.
- EEA: Reporting on Ambient Air Quality Assessment in the EU Member States 2008ETC/ACC Technical Paper 2010/11, 2010.
- Gietl, J., Lawrence, R., Thorpe, A., and Harrison, R.: Identification of brake wear particles and derivation of a quantitative tracer for brake dust at a major road, *Atmos. Environ.*, 44, 141–146, 2010.
- Harrison, R. M., Jones, A. M., and Barrowcliffe, R.: Field study of the influence of meteorological factors and traffic volumes upon suspended particle mass at urban roadside sites of differing geometries, *Atmos. Environ.*, 38, 6361–6369, 2004.
- Harrison, R. M., Beddows, D. C. S., Hu, L., and Yin, J.: Comparison of methods for evaluation of wood smoke and estimation of UK ambient concentrations, *Atmos. Chem. Phys.*, 12, 8271–8283, doi:10.5194/acp-12-8271-2012, 2012.
- Hodzic, A., Wiedinmyer, C., Salcedo, D., and Jimenez, J. L.: Impact of trash burning on air quality in Mexico City, *Environ. Sci. Technol.*, 1, 46, 4950–4957, 2012.
- Hu, C. W., Chao, M. R., Wu, K. Y., Chang-Chien, G. P., Lee, W. J., Chang, L. W., and Lee, W. S.: Characterization of multiple airborne particulate metals in the surroundings of a municipal waste incinerator in Taiwan, *Atmos. Environ.*, 37, 2845–2852, 2003.
- Karanasiou, A. A., Siskos, P. A., and Eleftheriadis, K.: Assessment of source apportionment by Positive Matrix Factorization analysis on fine and coarse urban aerosol size fraction, *Atmos. Environ.* 43, 3385–3395, 2009.
- Johansson, Ch., Norman, M., and Burman, L.: Road traffic emission factors for heavy metals. *Atmos. Environ.*, 43, 4681–4688, doi:10.1016/j.atmosenv.2008.10.024, 2008.
- Li, G., Lei, W., Bei, N., and Molina, L. T.: Contribution of garbage burning to chloride and PM<sub>2.5</sub> in Mexico City, *Atmos. Chem. Phys.*, 12, 8751–8761, doi:10.5194/acp-12-8751-2012, 2012.
- Lucarelli, F., Nava, S., Calzolari, G., Chiari, M., Udisti, R., and Marino, F.: Is PIXE still a useful technique for the analysis of at-



- ospheric aerosols? The LABEC experience, *X-Ray Spectrom.*, 40, 162–167, 2011.
- Marenco, F., Bonasoni, P., Calzolari, F., Ceriani, M., Chiari, M., Cristofanelli, P., D'Alessandro, A., Fermo, P., Lucarelli, F., Mazzei, F., Nava, S., Piazzalunga, A., Prati, P., Valli, G., and Vecchi, R.: Characterization of atmospheric aerosols at Monte Cimone, Italy, during summer 2004: source apportionment and transport mechanisms, *J. Geophys. Res.*, 111, D24202, doi:10.1029/2006JD007145, 2006.
- Moffet, R. C., de Foy, B., Molina, L. T., Molina, M. J., and Prather, K. A.: Measurement of ambient aerosols in northern Mexico City by single particle mass spectrometry, *Atmos. Chem. Phys.*, 8, 4499–4516, doi:10.5194/acp-8-4499-2008, 2008a.
- Moffet, R. C., Desyaterik, Y., Hopkins, R. J., Tavanski, A. V., Gilles, M. K., Wang, Y., Shutthanandan, V., Molina, L. T., Gonzalez, R., Johnson, K. S., Mugica, V., Molina, M. J., Laskin, A., and Prather, K. A.: Characterization of aerosols containing Zn, Pb, and Cl from an industrial region of Mexico City, *Environ. Sci. Technol.*, 42, 7091–7097, doi:10.1021/es7030483, 2008b.
- Moreno, T., Querol, X., Alastuey, A., de la Rosa, J., Sanchez-Campa, A., Minguillon, M. C., Pandolfi, M., Gonzalez-Castanedo, Y., Monfort, E., and Gibbons, W.: Variations in vanadium, nickel and lanthanoid element concentrations in urban air, *Sci. Total Environ.*, 408, 4569–4579, 2010.
- Moreno, T., Querol, X., Alastuey, A., Reche, C., Cusack, M., Amato, F., Pandolfi, M., Pey, J., Richard, A., Prévôt, A. S. H., Furger, M., and Gibbons, W.: Variations in time and space of trace metal aerosol concentrations in urban areas and their surroundings, *Atmos. Chem. Phys.*, 11, 9415–9430, doi:10.5194/acp-11-9415-2011, 2011.
- Muleski, G. E., Cowherd, C. J., and Kinsey J. S.: Particulate emissions from construction activities, *J. Air Waste Manage. Assoc.*, 55, 772–783, 2005.
- Nriagu, J. O. and Pacyna, J. M.: Quantitative assessment of worldwide contamination of air, water and soils by trace metals, *Nature*, 333, 134–139, 1988.
- Oliveira, C., Pio, C., Caseiro, A., Santos, P., Nunes, T., Mao, H., Luahana, L., and Sokhi, R.: Road traffic impact on urban atmospheric aerosol loading at Oporto, Portugal, *Atmos. Environ.*, 44, 3147–3158, 2010.
- Paatero, P. and Hopke, P. K.: Discarding or downweighting high-noise variables in factor analytic models. *Anal. Chim. Acta*, 490, 277–289, 2003.
- Pacyna, J. M. and Pacyna, E. G.: An assessment of global and regional emissions of trace metals to the atmosphere from anthropogenic sources worldwide, *Environ. Rev.*, 9, 269–298, 2001.
- Pant, P. and Harrison, R. M.: Critical Review of Receptor Modelling for Particulate Matter: A Case Study of India, *Atmos. Environ.*, 49, 1–12, 2012.
- Pastor, S. H., Allen, J. O., Hughes, L. S., Bhave, P., Cass, G. R., and Prather, K. A.: Ambient single particle analysis in Riverside, California by aerosol time-of-flight mass spectrometry during the SCOS97-NARSTO, *Atmos. Environ.*, 37, S239–S258, 2003.
- Pey, J., Perez, N., Castillo, S., Viana, M., Moreno, T., Pandolfi, M., Lopez-Sebastian, J. M., Alastuey, A., and Querol, X.: Geochemistry of regional background aerosols in the Western Mediterranean, *Atmos. Res.*, 94, 422–435, 2009.
- Pope, C. A. and Dockery, D. W.: Health effects of fine particulate air pollution: Lines that connect, *J. Air Waste Manage. Assoc.*, 56, 709–742, 2006.
- Polissar, A. V., Hopke, P. K., Paatero, P., Malm, W. C., and Sisler, J. F.: Atmospheric aerosol over Alaska. 2. Elemental composition and sources, *J. Geophys. Res.*, 103, 19045–19057, 1998.
- Prati, P., Zucchiatti, A., Tonus, S., Lucarelli, F., Mondo, P. A., and Ariola, V.: A testing technique of Streaker aerosol samplers via PIXE analysis, *Nuclear Instruments and Methods in Physics Research, Section B*, 138, 986–989, 1998.
- Putaud, J.-P., Van Dingenen, R., Alastuey, A., Bauer, H., Birmili, W., Cyrys, J., Flentje, H., Fuzzi, S., Gehrig, R., Hansson, H. C., Harrison, R. M., Herrmann, H., Hitznerberger, R., Hüglin, C., Jones, A. M., Kasper-Giebl, A., Kiss, G., Kousa, A., Kuhlbusch, T. A. J., Loschau, G., Maenhaut, W., Molnar, A., Moreno, T., Pekkanen, J., Perrino, C., Pitz, M., Puxbaum, H., Querol, X., Rodriguez, S., Salma, I., Schwarz, J., Smolik, J., Schneider, J., Spindler, G., Brink, H., Tursic, J., Viana, M., Wiedensohler, A., and Raes, F.: A European Aerosol Phenomenology – 3: Physical and chemical characteristics of particulate matter from rural, urban, and kerbside sites across Europe, *Atmos. Environ.*, 44, 1308–1320, 2010.
- Querol, X., Alastuey, A., Rodriguez, S., Plana, F., Mantilla, E., and Ruiz, C. R.: Monitoring of PM<sub>10</sub> and PM<sub>2.5</sub> around primary particulate anthropogenic emission sources. *Atmos. Environ.*, 35, 845–858, 2001.
- Querol, X., Pey, J., Minguillón, M. C., Pérez, N., Alastuey, A., Viana, M., Moreno, T., Bernabé, R. M., Blanco, S., Cárdenas, B., Vega, E., Sosa, G., Escalona, S., Ruiz, H., and Artífano, B.: PM speciation and sources in Mexico during the MILAGRO-2006 Campaign, *Atmos. Chem. Phys.*, 8, 111–128, doi:10.5194/acp-8-111-2008, 2008.
- Reche, C., Querol, X., Alastuey, A., Viana, M., Pey, J., Moreno, T., Rodríguez, S., González, Y., Fernández-Camacho, R., de la Rosa, J., Dall'Osto, M., Prévôt, A. S. H., Hueglin, C., Harrison, R. M., and Quincey, P.: New considerations for PM, Black Carbon and particle number concentration for air quality monitoring across different European cities, *Atmos. Chem. Phys.*, 11, 6207–6227, doi:10.5194/acp-11-6207-2011, 2011.
- Richard, A., Gianini, M. F. D., Mohr, C., Furger, M., Bukowiecki, N., Minguillón, M. C., Lienemann, P., Flechsig, U., Appel, K., DeCarlo, P. F., Heringa, M. F., Chirico, R., Baltensperger, U., and Prévôt, A. S. H.: Source apportionment of size and time resolved trace elements and organic aerosols from an urban courtyard site in Switzerland, *Atmos. Chem. Phys.*, 11, 8945–8963, doi:10.5194/acp-11-8945-2011, 2011.
- Salcedo, D., Onasch, T. B., Aiken, A. C., Williams, L. R., de Foy, B., Cubison, M. J., Worsnop, D. R., Molina, L. T., and Jimenez, J. L.: Determination of particulate lead using aerosol mass spectrometry: MILAGRO/MCMA-2006 observations, *Atmos. Chem. Phys.*, 10, 5371–5389, doi:10.5194/acp-10-5371-2010, 2010.
- Sanders, P. G., Xu, N., Dalka, T. M., and Maricq, M. M.: Airborne brake wear debris: size distributions, composition, and a comparison of dynamometer and vehicle tests, *Environ. Sci. Technol.*, 37, 4060–4069, 2003.
- Seinfeld, J. H. and Pandis, S. N.: *Atmospheric Chemistry and Physics: From Air Pollution to Climate Change*, 1st edition, J. Wiley, New York, USA, 1998.
- Solazzo, E., Cai, X., and Vardoulakis, S.: Modelling wind flow and vehicle-induced turbulence in urban streets, *Atmos. Environ.*, 42, 4918–4931, 2008.

- Sternbeck, J., Sjödin, Å., and Andréasson, K.: Metal emissions from road traffic and the influence of resuspension. A results from two tunnel studies, *Atmos. Environ.*, 36, 4735–4744, 2002.
- Tan, P. V., Fila, M. S., Evans, G. J., and Jervis, R. E.: Aerosol laser ablation mass spectrometry of suspended powders from PM sources and its implications to receptor modelling, *J. Air Waste Manage.*, 52, 27–40, 2002
- Viana, M. M., Querol, X., Alastuey, A., Iburguchi, J. I., and Menendez, M.: Identification of PM sources by principal component analysis (PCA) coupled with meteorological data, *Chemosphere*, 65, 2411–2418, 2006.
- Walsh, D. C., Chillrud, S. N., Simpson, H. J., and Bopp, R. F.: Refuse incinerator particulate emissions and combustion residues for New York City during the 20th century, *Environ. Sci. Technol.*, 35, 2441–2447, 2001.